Clay Minerals, (2018) **53**, 1–15

Removal of Cu^{2+} and Ni^{2+} ions from aqueous solutions by adsorption onto natural palygorskite and vermiculite

A. BOURLIVA[1,*], A. K. SIKALIDIS[2], L. PAPADOPOULOU[1], M. BETSIOU[3], K. MICHAILIDIS[1], C. SIKALIDIS[3] AND A. FILIPPIDIS[1]

[1] *Department of Mineralogy-Petrology-Economic Geology, School of Geology, Aristotle University of Thessaloniki, 54124 Thessaloniki, Greece*

[2] *Istanbul Yeni Yuzyil University, Department of Nutrition and Dietetics, Istanbul, Turkey*

[3] *Department of Chemical Engineering, School of Engineering, Aristotle University of Thessaloniki, 54124 Thessaloniki, Greece*

(*Received 4 May 2017; revised 18 January 2018; Associate Editor: H. Stanjek*)

ABSTRACT: The efficiency of two low-cost, abundant and natural clay minerals, palygorskite and vermiculite, in terms of reducing the concentation of Cu^{2+} and Ni^{2+} ions was evaluated here. Natural clay minerals were characterized by X-ray powder diffraction (XRD), scanning electron microscopy (SEM), Fourier Transform Infrared Spectroscopy (FTIR), BET specific surface area and pore-diameter analysis. Batch-type experiments were performed and various parameters, *i.e.* pH, clay amount, contact time and initial metal concentration, that affect adsorption processes were investigated. The adsorption of Cu^{2+} and Ni^{2+} ions is pH-dependent, while minor clay quantities were sufficient to achieve high removal efficiencies. Adsorption equilibrium occurred in 60 min and the adsorption kinetics were better described by pseudo-second-order kinetics. Experimental results were analysed by the Langmuir, Freundlich, Dubinin–Radushkevich (D–R), Temkin and Halsey isotherm equations. The release of exchangeable cations (*i.e.* Ca^{2+}, Mg^{2+}, Na^{+} and K^{+}) was examined to verify an ion-exchange mechanism.

KEYWORDS: palygorskite, vermiculite, adsorption, ion exchange, isotherms, trace elements.

Heavy metals pose a serious environmental concern owing to their toxicity and abundance. They enter into aquatic environments, causing various health problems to human beings and animals because of their non-degradable, persistent and accumulative nature (Fu & Wang, 2011; Uddin, 2017). However, some heavy metals are essential, being vital to the health of a vast variety of entities (humans, plants, animals and microorganisms), although they can cause harm in excessive concentrations (Hu, 2002). For instance, in humans, Cu is involved in a series of metabolic processes as an important enzymatic co-factor, while Ni is essential for microorganisms that colonize the human gut (Brewer, 2003). However, evidence of any distinct benefit from nickel supplementation in human tissues is lacking (Brewer, 2003, 2014). On the other hand, evidence of a relationship between high levels of copper and Alzheimer's disease and potential carcinogenesis has been found (Harris, 2003; Magave *et al.*, 2012), while nickel is associated with a vast array of diseases and is considered to be one of the most common contact sensitizers causing allergic dermatitis (Kurniawan *et al*., 2006; Sharma, 2006, 2013).

*E-mail: annab@geo.auth.gr
https://doi.org/10.1180/clm.2017.1

Several techniques such as chemical precipitation, evaporation, solvent extraction, ion exchange, electrochemical treatment and membrane filtration technologies, *etc*., have been utilized for heavy-metal removal. Adsorption is a suitable technique with competitive advantages compared to other techniques, including low cost, ease of operation, efficiency and effectiveness (Cheremisinoff, 1995; Bhattacharya *et al.,* 2006), which can be amplified when low-cost adsorbents are utilized. Various clays and clay minerals have attracted attention as effective adsorbents for the efficient removal of heavy-metal ions from aqueous solutions (Srinivasan, 2011; Uddin, 2017 and references therein). Clays have advantages compared to other adsorbents because they are low cost, widespread, have large specific surface areas and significant potential for ion exchange (Malamis & Katsou, 2013; Hojati & Landi, 2015; Uddin, 2017).

Palygorskite is a Mg-Al silicate mineral with a three-dimensional, chain-like inverted crystal structure that gives rise to a fibrous morphology. Its open-channel structure that is simultaneously negatively charged due to isomorphic substitutions, along with the large specific surface area, ensure its large adsorption capacity (Murray, 1999). On the other hand, vermiculite is a 2:1 Al-Fe-Mg silicate mineral with hydrated exchangeable cations compensating the negative layer charge, which contribute to high cation-exchange capacity (CEC) (Xueyi & Inoue, 2003; Stylianou *et al.,* 2007).

In this study, the ability of palygorskite and vermiculite to adsorb Cu^{2+} and Ni^{2+} ions from aqueous solutions was investigated. More specifically, the effects of several operating parameters such as contact time, clay amount, solution pH and initial metal concentration were investigated. Furthermore, kinetics studies were employed to propose plausible adsorption mechanisms.

MATERIALS AND METHODS

Clay minerals

The natural clays used in the present study were palygorskite (ATP) mined from the Ventzia basin, Grevena (western Macedonia, Greece), and vermiculite (VRM) from the Askos area (northern Greece). The palygorskite sample was considered to be the alteration product of primary ultramafic rocks of the Vourinos complex (Kastritis *et al.,* 2003), while vermiculite was considered to be a product of mica alteration in serpentinized ultramafic rocks along their contacts with two-mica gneisses (Tsirambides & Michailidis, 1999). The samples were ground, sieved to obtain the <63 μm particle-size fraction, and used in adsorption experiments without chemical treatment.

Characterization of natural clays

Mineralogical characterization of the clay samples was performed by X-ray powder diffraction (XRPD) using a Philips PW1710 diffractometer. Ni-filtered CuKα radiation was used energized to 35 kV and 25 mA, in the range 3–63°2θ at a scan speed of 1.2°/min. The Fourier Transform Infrared Spectra (FTIR) of the studied clays were recorded (4000–400 cm^{-1}) with a Perkin-Elmer FTIR Spectrum 1000 spectrometer at a resolution of 4 cm^{-1} using the KBr pellet technique. A scanning electron microscope (JEOL JSM-840A) was used to analyse the morphological characteristics of the studied clays before and after adsorption. Spot elemental analyses and X-ray mapping were obtained using an X-ray energy dispersive spectrometer-EDX (INCA 300). The chemical composition of the clays was determined following a three acid (HF, H_2SO_4 and $HClO_3$) digestion in autoclaves according to Bourliva *et al.* (2013a). The CEC was determined after saturation with sodium (sodium acetate solution buffered at pH 8.2), removal of the excess sodium with ethanol, and replacement of exchangeable sodium with ammonium acetate solution buffered at pH = 7 (Alexiades & Jackson, 1966). The specific surface area, pore volume and pore size of the clays were determined from N_2 adsorption-desorption isotherms using a surface area and porosimetry analyzer (Micromeritics, TriStar 3000). The N_2 adsorption-desorption isotherms were measured at 77 K after outgassing the samples at 250°C for 18 h.

Adsorption experiments

The experimental adsorption equilibrium data were obtained in batch-adsorption mode. The experimental procedure was described previously by Bourliva *et al.* (2013b, 2015). In brief, 100 mL of a single metal solution and a pre-weighed clay amount were poured into centrifugal vials and placed on a vertical rotary shaker (10 turns/min) for a desired time interval for equilibrium to be attained, centrifuged at 3000 rpm for 15 min, and the final concentration of each metal was determined by Atomic Absorption Spectroscopy (AAS). Metal solutions with known initial metal concentrations were prepared at a specific pH by mixing proper volumes of 0.01 M HNO_3 and NaOH solutions. The pH was monitored before and after adsorption. All measurements

https://doi.org/10.1180/clm.2017.1 Published online by Cambridge University Press

were made in duplicate and the average values were reported. Blank experiments both without clay and without metal were also performed. The experimental conditions maintained for the different operating parameters such as pH of suspension, adsorbent amount, contact time and metal concentration were as follows:

(1) Effect of pH: Clay dosage 1 g L^{-1}, initial metal concentration 50 mg L^{-1}, temperature 303 K, contact time 120 min, pH range 2.0–6.0 for Cu^{2+} and 2.0–8.0 for Ni^{2+} ions
(2) Effect of clay dosage: Initial metal concentration 50 mg L^{-1}, temperature 303 K, pH_{Ni} 4.85 and pH_{Cu} 5.10, contact time 120 min, adsorbent dosage 1, 3, 5, 7, 9, 10 g L^{-1}
(3) Kinetic study: Clay dosage 1 g L^{-1}, initial metal concentration 50 mg L^{-1}, temperature 303 K, pH_{Ni} 4.85 and pH_{Cu} 5.10, contact time 20, 40, 60, 90, 120, 180, 240, 360 min
(4) Adsorption isotherms-counterbalanced ions: Clay amount 1 g L^{-1}, temperature 303 K, pH_{Ni} 4.85 and pH_{Cu} 5.10, contact time 120 min, initial metal concentration 5, 10, 25, 50, 75, 100, 250 mg L^{-1}. The concentrations of Ca^{2+}, Mg^{2+}, K^{+} and Na^{+} were measured in the supernatant solutions after the experiments.

The amount, q_e, of the Cu^{2+} and Ni^{2+} ions adsorbed per unit mass of the adsorbent and the extent of removal (%) were calculated using the following equations:

$$q_e = \frac{(C_o - C_e)V}{m} \quad (1)$$

$$\%\text{Removal} = \frac{(C_o - C_e)}{C_o} 100 \quad (2)$$

where C_o (mg L^{-1}) is the initial Cu^{2+} or Ni^{2+} concentration in the solution, C_e (mg L^{-1}) is the concentration of Cu^{2+} or Ni^{2+} in the solution at equilibrium, m is the clay mass (g) and V is the solution volume (L).

RESULTS AND DISCUSSION

Clay characterization

Examination of the XRD patterns (Fig. 1) showed that ATP consists mainly of palygorskite (92%), minor nontronite (5%) and quartz (3%), while in the VRM sample, vermiculite (72%) along with mixed-layer biotite-vermiculite (hydrobiotite, 17%) and chlorite-vermiculite (corrensite, 11%) were detected. The XRD results were confirmed by the FTIR analysis (Fig. 2). The FTIR spectrum (Fig. 2) of ATP is typical of Fe-rich palygorskite exhibiting two bands at 3612 and 3552 cm^{-1} attributed to the structural OH-stretching vibrations of Al and Fe, while the stretching vibration at 3418 cm^{-1} was due to water in the palygorskite channels (Chahi *et al.,* 2002; Suárez & García-Romero, 2006). Also, a very characteristic Si–O stretching pattern for palygorskite was presented with a high-frequency component at 1198 cm^{-1} and a doublet of low-frequency vibrations at 1030 and 988 cm^{-1} (Mendelovici, 1973; Frost *et al.,* 2001; Madejová *et al.,* 2011). The structural OH-stretching band at 3612 cm^{-1} along with the well-defined Al_2OH deformation band at 915 cm^{-1} and a slight inflection near 862 cm^{-1} (AlMgOH) reflect the dominantly dioctahedral character of the ATP sample (Madejová & Komadel, 2001). Additionally, the bands at 3552 cm^{-1} and 820 cm^{-1} assigned to Fe_2OH stretching and bending, respectively, validated the presence of dioctahedral smectite (nontronite) in the ATP sample (Christidis *et al.,* 2010) and not trioctahedral smectite

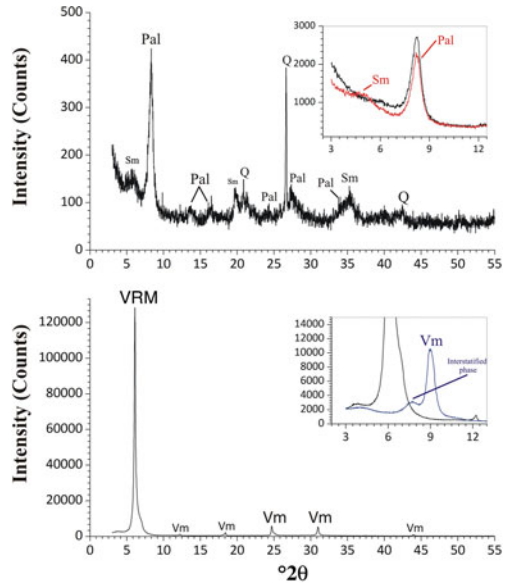

FIG. 1. XRD patterns of the natural clays studied: palygorskite (upper) and vermiculite (lower). Inset are the patterns of the oriented (black line), glycolated (red line) and heated (blue line) samples. Pal: palygorskite (JCPDS card No. 31-0783), Sm: smectite (JCPDS card No. 29-1497), Q: quartz (JCPDS card No. 46-1045), VRM: vermiculite (JCPDS card 16-0613).

https://doi.org/10.1180/clm.2017.1 Published online by Cambridge University Press

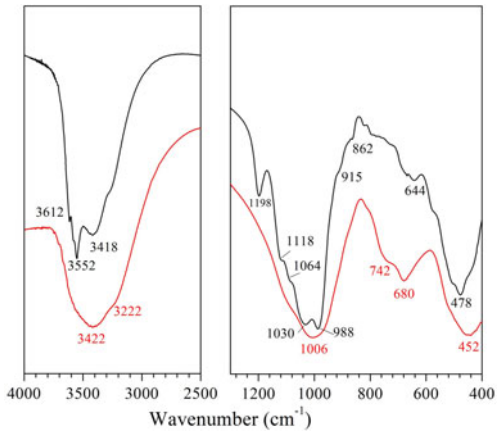

FIG. 2. FTIR spectra of the natural clays studied: palygorskite (ATP, black line) and vermiculite (VRM, red line).

(saponite) as was assumed in earlier studies (Kastritis *et al.,* 2003). Quartz admixture (790 cm^{-1}) was also revealed in ATP spectra. On the other hand, the spectrum of vermiculite (VRM) showed a strong, broad OH-stretching band at 3422 cm^{-1} characteristic of mixed-layer vermiculite samples (Muiambo *et al.,* 2010). The band at 1006 cm^{-1} was ascribed to a Si-O-Si stretching.

The SEM images show a typical fibrous texture for attapulgite (ATP), while in the VRM, the mixed-layer phases were presented as brighter and darker regions (Fig. 3). The chemical compositions of the natural clays used, the CEC values and the textural properties of the clays are listed in Table 1.

Effects of various parameters on the ability of adsorbents to remove Cu and Ni

Effect of pH. The initial pH value of the metal aqueous solution is a significant factor in the adsorption process and this controls the uptake of the metal ions at the adsorbent–clay interfaces. The effect of solution pH was investigated in the range 2–6 for copper and 2–8 for nickel, which avoids metal precipitation in hydroxide forms and maintains their cationic species (Bayat, 2002; Sen Gupta & Bhattacharyya, 2008); results are shown in Fig. 4. The adsorption of Cu^{2+} and Ni^{2+} ions was highly pH-dependent, and increased adsorption capacities, q_e (mg g^{-1}) with increasing pH were observed. As far as the efficiency of the studied clays is concerned, vermiculite took up more Cu^{2+} and Ni^{2+} ions at a given pH than palygorskite. The differences in amount adsorbed with pH, and particularly the reduced removal efficiencies for all studied cases at low pH, could be ascribed to: (1) the antagonism between the metal and H_3O^+ ions for the vacant adsorption sites on clay surfaces at substantially low pH values; and (2) surface protonation reactions lead to positively charged clay surfaces at lower pH and hence to increased repulsion forces between metal ions and clay surfaces, which prevent metal ions from accessing the surface binding sites. This ultimately leads to lower adsorption efficiency (Mathialagan & Viraraghavan, 2003; Sen Gupta & Bhattacharyya, 2008).

Effect of clay amount. The effect of clay amount was studied by variation of dosages from 0.1 to 1 g L^{-1} and the results are presented in Fig. 5. In VRM a dose of 5 g L^{-1} exhibited removal efficiency of >90% for both Cu^{2+} and Ni^{2+} ions, while for ATP larger amounts are necessary to achieve satisfactory removal efficiencies. Generally, the adsorption extent, calculated as the % removal of Cu^{2+} and Ni^{2+} ions, increased with increasing clay dosage. This might be ascribed to the larger surface area and more binding sites available as the clay amount increased (Liu & Zhou, 2010; Sen & Gomez, 2011). A reverse trend was observed in adsorption capacity (q_e) which decreased gradually with the increase in clay

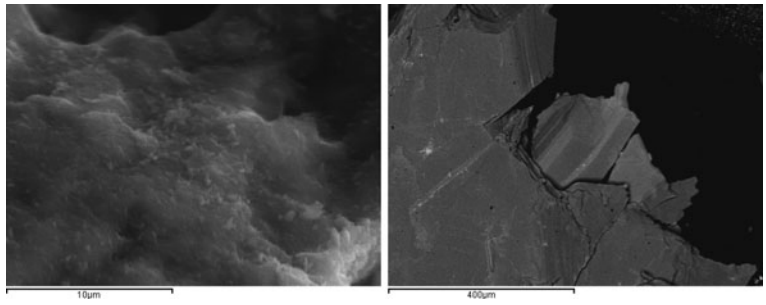

FIG. 3. SEM images of the palygorskite (ATP, left) and vermiculite (VRM, right).

https://doi.org/10.1180/clm.2017.1 Published online by Cambridge University Press

TABLE 1. Chemical composition (wt. %), CEC and textural properties of the natural clays studied.

	SiO_2	Al_2O_3	TiO_2	MnO	Fe_2O_3	Cr_2O_3	MgO	CaO	Na_2O	K_2O	P_2O_5	LOI[1]
ATP	58.83	8.66	0.40	0.07	7.96	0.17	9.97	0.65	0.18	0.49	0.02	12.36
VRM	36.99	12.81	1.01	0.13	10.82	0.10	20.03	0.15	bdl[2]	0.13	0.02	17.69

	CEC (meq/100 g)	Surface area (m^2/g)	Pore volume (cm^3/g)	Pore size (nm)
ATP	57.6	148.23	0.503	13.58
VRM	128.3	16.99	0.052	12.18

[1] LOI: loss on ignition, [2] bdl: below detection limit.

amount. This might be explained by: (1) the large clay quantities efficiently diminish the saturation of the adsorption sites resulting in the reduction of covered sites per unit mass and therefore to a lesser adsorption capacity; and (2) higher clay dosages led to aggregation phenomena which result in lower total surface area, and increased divisional path length, both of which lead to decreased adsorption capacity (Shukla *et al.,* 2002).

Effect of contact time and adsorption kinetics. The effect of contact time on the adsorption of Cu^{2+} and Ni^{2+} ions was investigated at various time intervals in the range 20–360 min and the results are presented in Fig. 6. The removal of Cu^{2+} and Ni^{2+} ions increased rapidly in both clays in the first 20 min of adsorption, while negligible differences in the removal of metal ions were noted after ~60 min of contact, indicating that adsorption equilibrium was established. This might be attributed to the high rate at which adsorption takes place on the free surface in the first stage of adsorption, while, as the sites were filled with the metal ions, the rate decreased (Srivastava *et al.,* 2008). The adsorption capacities recorded for vermiculite were significantly higher than those for palygorskite, indicating its better applicability.

In order to investigate the adsorption mechanism, and particularly the adsorption rate, various kinetic models (data not shown) were used. The best-fit kinetic model was evaluated by the linear coefficient of determination (R^2) and the experimental ($q_{e,exp}$) and calculated ($q_{e,cal}$) adsorption capacities. Larger R^2 values and the smaller variations in q_e values were observed for a pseudo-second-order kinetic model

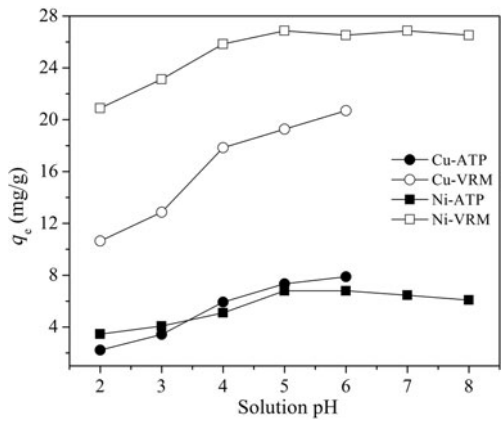

FIG. 4. Effect of pH on Cu^{2+}, and Ni^{2+} adsorption by the natural clays studied. Contact time: 120 min; adsorbent dosage: 1 g L^{-1}; initial metal concentration: 50 mg L^{-1}.

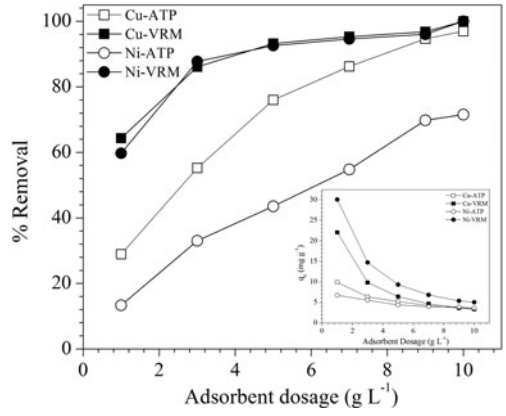

FIG. 5. Effect of adsorbent dosage on Cu^{2+} and Ni^{2+} adsorption by the natural clays studied. Contact time: 120 min; initial pH: pH_{Cu} 5.10, pH_{Ni} 4.85; initial metal concentration: 50 mg L^{-1}.

https://doi.org/10.1180/clm.2017.1 Published online by Cambridge University Press

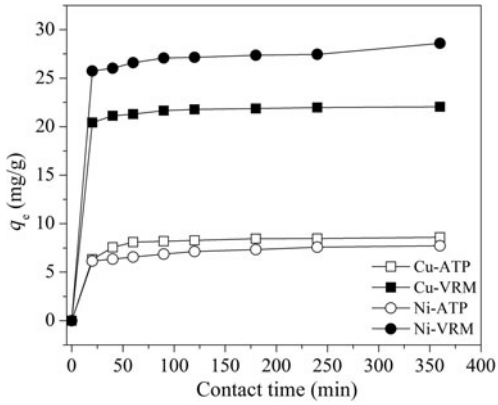

FIG. 6. Effect of contact time on Cu^{2+}, and Ni^{2+} adsorption by the natural clays studied. Initial metal concentration: 50 mg L^{-1}; initial pH: pH_{Cu} 5.10, pH_{Ni} 4.85; adsorbent dosage: 1 g L^{-1}.

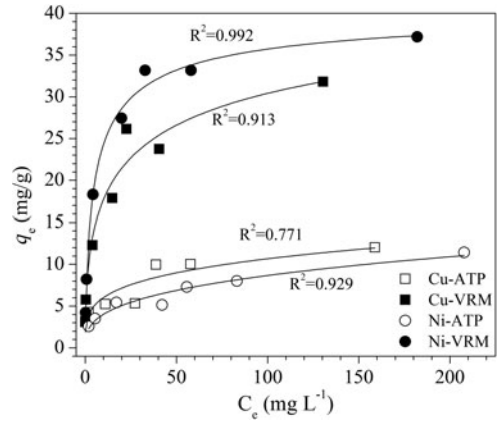

FIG. 7. Adsorption isotherms for Cu^{2+} and Ni^{2+} ions. The lines represent a non-linear fit of the Langmuir isotherm.

(Table 2), which is expressed by equation 3 (Ho & McKay, 1998) as follows:

$$\frac{t}{q_t} = \frac{1}{(k_2 q_e^2)} + \frac{1}{q_e} t \qquad (3)$$

where q_t and q_e are the adsorption capacities at time t (min) and equilibrium time (mg g^{-1}), respectively and k_2 (g mg^{-1} min^{-1}) is the rate constant of the pseudo-second-order adsorption, which better described the experimental kinetic data.

Adsorption isotherms

The experimental data obtained from the adsorption isotherm studies are essential for assessment of the surface properties and the affinity of an adsorbent for a specific sorbate, both of which are critical in optimizing its usage. The adsorption isotherms for Cu^{2+} and Ni^{2+} are presented in Fig. 7. The increase in the initial metal concentration resulted in an increase of the adsorption capacity. The isotherms were of L-type (Giles *et al.,* 1974) indicating a high affinity between sorbent and solute. The Cu^{2+} and Ni^{2+} ions adsorbed per unit mass of the natural clays studied were expressed as a percentage of the CEC and the results are given in Fig. 8. Even for an initial Cu^{2+} concentration of 250 mg/L, almost 66% and 78% of the available exchangeable sites of ATP and VRM samples were covered, respectively. Correspondingly, almost 64% and 98% of the available sites of ATP and VRM were covered with Ni^{2+}, respectively.

With a view to understanding the mechanism of Cu^{2+} and Ni^{2+} adsorption onto the ATP and VRM samples, the experimental data obtained were tested with the Langmuir, Freundlich, Dubinin–Radushkevich (D–R), Temkin and Halsey isotherm models. The adsorption isotherm models equations are shown below (equations 4–8):

$$q_e = \frac{q_m b C_e}{(1 + bC_e)} \qquad (4)$$

TABLE 2. Parameters of the pseudo-second-order kinetic model for adsorption of Cu^{2+} and Ni^{2+} ions by the natural clays studied.

		q_e (exp) mg/g	$k_{2\times}10^2$ g $mg^{-1}min^{-1}$	q_e mg/g	R^2
Cu^{2+}	ATP	8.60	1.81	8.74	0.999
	VRM	22.05	2.14	22.16	0.999
Ni^{2+}	ATP	7.72	1.13	7.94	0.997
	VRM	28.60	0.52	29.41	0.998

https://doi.org/10.1180/clm.2017.1 Published online by Cambridge University Press

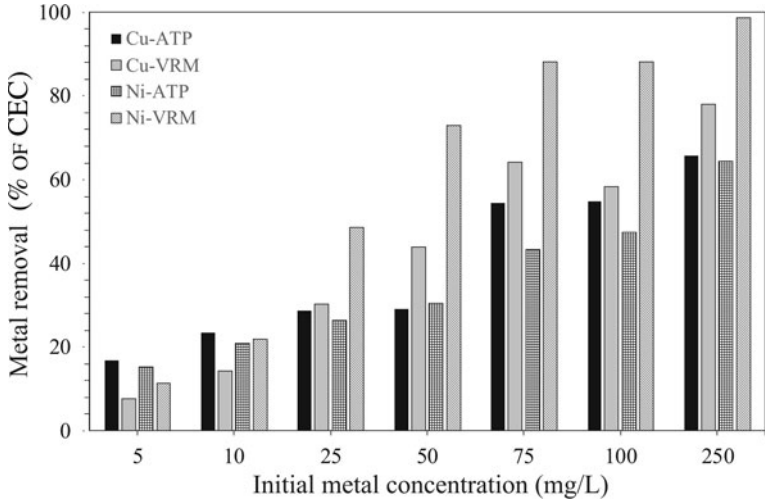

FIG. 8. The amounts of Cu^{2+} and Ni^{2+} ions adsorbed in different initial concentrations, expressed as a percentage (%) of the CEC of the natural clays studied.

where q_e (mg g^{-1}) is the adsorption capacity at equilibrium, C_e (mg L^{-1}) is the concentration of the sorbate at equilibrium, b (L mg^{-1}) is the Langmuir equilibrium constant associated to the energy of adsorption and q_m (mg g^{-1}) denotes the theoretical Langmuir monolayer adsorption capacity.

$$q_e = K_F C_e^{1/n} \quad (5)$$

where K_F (mg^{1-n} L^n g^{-1}) and n (dimensionless) are Freundlich constants related to adsorption capacity and sorption intensity, respectively.

$$q_e = Q_m e^{-\beta\varepsilon^2} \quad (6)$$

where Q_m (mol g^{-1}) is the Dubinin–Radushkevich monolayer capacity, β (mol^2 kJ^{-2}) is a constant related to sorption energy, and ε represents the Polanyi potential constant which is related to the equilibrium concentration and is given as $\varepsilon = RT\ln(1+\frac{1}{C_e})$, where R is the gas constant ($8.314.10^{-3}$ kJ mol^{-1} K^{-1}) and T is the absolute temperature (K). Constant β gives the mean adsorption energy, E, of sorption per molecule of the sorbate when it is transferred to the surface of the solid from infinity in the solution and can be computed as $E = \frac{1}{\sqrt{2\beta}}$

$$q_e = B_T \ln(K_T C_e) \quad (7)$$

where B_T (J mol^{-1}) is related to the heat of adsorption and is given as $B_T = \frac{RT}{b_T}$, while b_T is the Temkin isotherm constant and K_T (L mg^{-1}) is the equilibrium binding constant.

$$q_e = e\left[\frac{(\ln K_H - \ln C_e)}{n_H}\right] \quad (8)$$

where K_H and n_H are the Halsey isotherm constants.

The linear coefficient of determination, R^2, was used to confirm the good fitness of each isotherm model to the experimental data, and the values along with the isotherms' parameters are presented in Table 3. The highest values of R^2 were observed for the Langmuir isotherm with the exception of Cu^{2+} adsorption onto VRM which follows the Freundlich isotherm model. The Langmuir equilibrium coefficient, b, was large with values of 42–94 L g^{-1} (Table 3) for the metal-ATP systems and even larger (130–203 L g^{-1}) for the metal ion-VRM systems. The higher value of b (203 L g^{-1}) for the adsorption of Ni^{2+} ions onto vermiculite showed that the interactions were stronger between nickel ions and vermiculite. The maximum adsorption capacity q_m was 12.53 mg g^{-1} and 32.68 mg g^{-1} for Cu^{2+} for ATP and VRM, respectively, while for Ni^{2+} ions it was 11.57 mg g^{-1} and 37.85 mg g^{-1}, respectively for ATP and VRM. The maximum adsorption capacities determined were higher in VRM than in ATP for both the Cu^{2+} and Ni^{2+} ions. Although the different experimental conditions applied make direct comparison between various adsorbents difficult, the adsorption capacities of the natural clays utilized in this study were notably higher than values reported from similar

https://doi.org/10.1180/clm.2017.1 Published online by Cambridge University Press

TABLE 3. Adsorption isotherm models and parameter values for the adsorption of Cu^{2+} and Ni^{2+} ions on the studied clays.

Isotherm model	Linearized equation		Parameter values			
			Cu(II)		Ni(II)	
			ATP	VRM	ATP	VRM
Langmuir	$\frac{C_e}{q_e} = \frac{1}{q_m b} + \frac{C_e}{q_m}$	q_m (mg g^{-1})	12.53	32.68	11.57	37.85
		b (L mg^{-1})	0.094	0.130	0.042	0.203
		R_L	0.068	0.050	0.141	0.033
		R^2	**0.984**	0.983	**0.992**	**0.998**
Freundlich	$\log q_e = \log K_F + \frac{1}{n}\log C_e$	K_F (mg^{1-n} L^n g^{-1})	4.20	8.00	3.49	11.39
		n	5.27	3.41	5.20	3.48
		R^2	0.928	**0.999**	0.924	0.979
Dubinin–Radushkevich	$\ln q_e = \ln q_m - \beta\varepsilon^2$	Q_m (mol g^{-1})	14.02	50.15	17.63	80.10
		β (mol^2 kJ^{-2})	0.0015	0.0023	3.04×10^{-3}	2.91×10^{-3}
		E (kJ mol^{-1})	15.26	14.74	12.82	13.11
		R^2	0.872	0.995	0.971	0.981
Temkin	$q_e = B_1 \ln K_T + B_1 \ln C_e$	B_T (J mol^{-1})	1.181	3.429	1.022	4.448
		b_T	2097.15	722.53	2425.07	557.00
		K_T (L mg^{-1})	43.642	23.198	36.66	32.88
		R^2	0.828	0.927	0.799	0.974
Halsey	$\ln q_e = \left[\left(\frac{1}{n_H}\right)\ln K_H\right] - \frac{1}{n_H}\ln C_e$	n_H	5.27	3.41	3.29	3.07
		K_H	1934.32	1210.35	10.82	839.32
		R^2	0.928	**0.999**	0.990	0.944

Significant R^2 values are marked in bold.

TABLE 4. Reported results on the adsorption capacities of various clay minerals for Cu^{2+} and Ni^{2+} ions.

Sorbent	Experimental conditions			Adsorption capacity (mg/g)		Reference
	pH	Temperature (°C)	Soil/liquid (g/L)	Cu	Ni	
Attapulgite	5	30	1	12.53	11.57	This study
Vermiculite				32.68	37.85	This study
Bentonite						Bourliva *et al.* (2015)
Bentonite		25	10	17.87	13.97	Liu & Zhou (2010)
Bentonite	5	25	15		13.97	Tahir & Rauf (2003)
Bentonite	7	25	4	44.84		Veli & Alyüz (2007)
Bentonite				32.17		Eren and Afsin (2008)
Bentonite	6	25	2	42.41		Eren (2008)
Ca-bentonite				7.7	6.3	Alvarez-Ayuso & Garcia-Sanchez (2003)
Ca-bentonite	5.7	25	4	1.98		Ding *et al.* (2009)
Kaolinite	5.5	30	2		7.1	Sen Gupta & Bhattacharyya (2008)
Kaolinite		30	25	1.22	0.9	Jiang *et al.* (2010)
Kaolinite		25	10	10.79	1.67	Yavuz *et al.* (2003)
Kaolinite				9.81		Al-Makhadmeh & Batiha (2016)
Montmorillonite	5.5			3.04	3.63	Abollino *et al.* (2008)
Montmorillonite	5.5	30	2		21.14	Sen Gupta & Bhattacharyya (2008)
Montmorillonite		25	20	7.62	12.89	Ijagbemi *et al.* (2009)
Montmorillonite			20		4.85	De Pablo *et al.* (2011)
Na-bentonite				30	24.2	Alvarez-Ayuso & Garcia-Sanchez (2003)
Na-bentonite	5.7	25	4	11.17		Ding *et al.* (2009)
Na-montmorillonite	6	25	5	58.47	48.54	Baker (2009)
Na-montmorillonite	6.5	25	6		10.65	Ijagbemi *et al.* (2010)
Na-montmorillonite	4.7	25	4	33.6		Özdemir & Yapar (2009)
Natural clay	6	25	1	17.89		Sdiri *et al.* (2014)
Palygorskite	7	25	1	30.67	33.44	Potgieter *et al.* (2006)
Vermiculite	4.5	25	60	3.28	0.32	Covelo *et al.* (2007)
Vermiculite	5.5			20.61	25.33	Abollino *et al.* (2008)
Vermiculite		25	1.25	43.67		El-Bayaa *et al.* (2009)

studies (Table 4). The separation factor, R_L, values calculated by the equation $R_L=1/(1+bC_0)$, where C_0 (mg L^{-1}) is the initial Cu^{2+} or Ni^{2+} concentration in the solution and b (L mg^{-1}) is the Langmuir constant, varied between 0.33 and 0.141 indicating favourable adsorption.

The Freundlich isotherm model, based on multilayer adsorption, exhibited good applicability ($R^2 = 0.924$–0.999). The estimated Freundlich adsorption constant (K_F) was higher for vermiculite (Cu^{2+}: 8.00, Ni^{2+}: 11.39 mg^{1-n} L^n g^{-1}) compared to that of palygorskite (Cu^{2+}: 4.20, Ni^{2+}: 3.49 mg^{1-n} L^n g^{-1}). This is in accordance with the experimental results in which vermiculite exhibited higher adsorption capacities than palygorskite. The Freundlich coefficient *n* values ranging from 1 to 10 (3.41–5.27) support the favourable adsorption of Cu^{2+} and Ni^{2+} ions onto the studied natural clays.

The D–R model described the experimental data well with the exception of Cu^{2+} adsorption onto ATP which presented a lower R^2 value (0.872) (Table 3). Within D–R parameters, the mean free energy (*E*) offers valuable information on the mechanism of adsorption. The *E* values were >8 kJ mol^{-1} (range 12.82–18.26 kJ mol^{-1}) in all cases, suggesting the dominance of chemical adsorption of Cu^{2+} and Ni^{2+} ions onto ATP and VRM. The comparison of D–R and Langmuir models' maximum monolayer capacity showed that the Langmuir model fitted the experimental data better than D–R isotherm. The Langmuir parameter (q_m) was closer to the experimental capacity determined compared with the corresponding D–R parameter (Q_m) which is higher than the experimental capacity value determined. Consequently, the Langmuir model explained better the Cu^{2+} and Ni^{2+} ions' adsorption onto the studied natural clays than the Dubinin–Radushkevich model.

The Temkin isotherm (data not shown) provides a close fit to the data for adsorption of Cu^{2+} and Ni^{2+} onto vermiculite, but the experimental data for the adsorption of the metal ions studied onto ATP did not fit well in the concentration range studied (Table 3). The values of the Temkin constants B_T, b_T and K_T are listed in Table 2. The B_T values which are indicative of

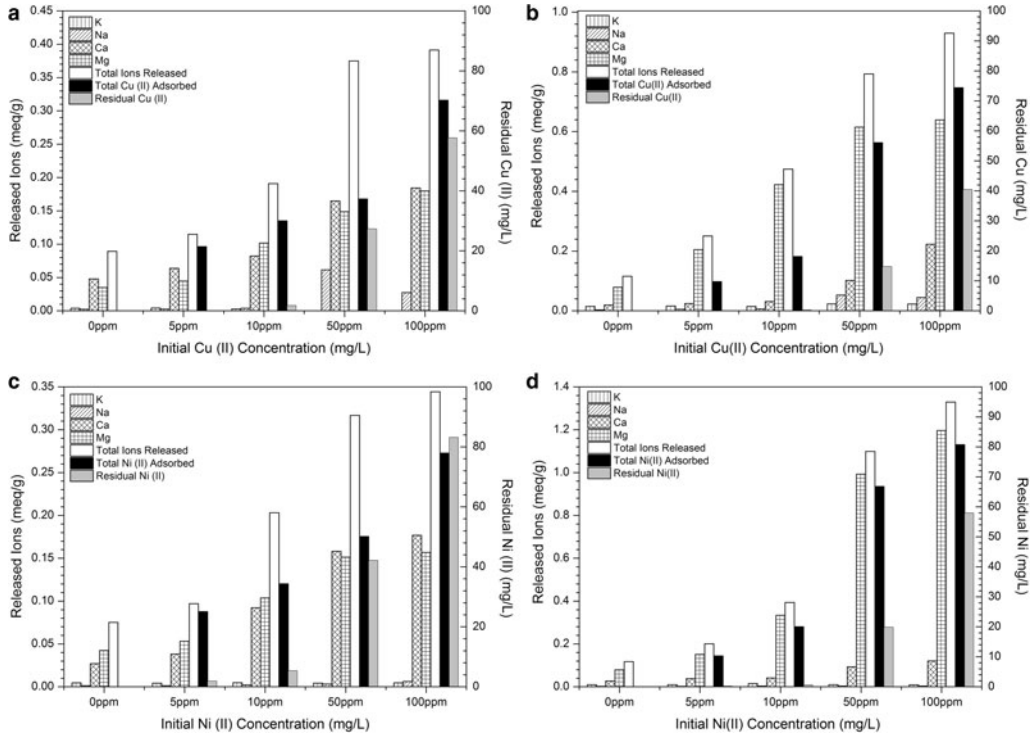

FIG. 9. Concentrations of released K^+, Na^+, Ca^{2+}, Mg^{2+} ions and total released cations (sum of $K^+ + Na^+ + Ca^{2+} + Mg^{2+}$ ions) during Cu^{2+} (up), and Ni^{2+} (down) adsorption (adsorbed-residual) by palygorskite (a, c) and vermiculite (b, d). The contact time applied was 120 min. The measured CECs were ~0.58 meq/g for ATP and ~1.28 meq/g for VRM.

https://doi.org/10.1180/clm.2017.1 Published online by Cambridge University Press

the heat of metal adsorption onto the studied natural clays were positive (1.022–4.448 J mol^{-1}) suggesting an endothermic adsorption reaction. On the other hand, the Halsey isotherm plots for the adsorption of Cu^{2+} and Ni^{2+} ions onto the studied natural clays (data not shown) exhibited high R^2 values (0.928–0.998) indicating a good fit of the experimental data and an accurate description of the sorption behaviour of Cu^{2+} and Ni^{2+} ions onto the studied clays (ATP and VRM) by the Halsey isotherm. The n_H values of the adsorption of Cu^{2+} ions onto ATP and VRM were 5.27 and 3.41, respectively, while those for the adsorption of Ni^{2+} ions were 3.29 and 3.07, respectively, suggesting that the adsorbed molecules may form multilayers (Tang *et al.,* 2003).

Evaluation of adsorption mechanism

The retention of Cu^{2+} and Ni^{2+} ions by the clays is clearly an ion exchange process which is validated by the determination of Ca^{2+}, Mg^{2+}, Na^+ and K^+ ions released during Cu and Ni adsorption, in relation to the initial concentrations (Fig. 9). Also, the total release of positively charged ions (sum of Ca^{2+}, Mg^{2+}, Na^+ and K^+ ions) from the two clay adsorbents along with the total adsorbed and the residual Cu^{2+} and Ni^{2+} ions are shown.

Briefly, in both the ATP and VRM clays, the amounts of Na^+ and K^+ ions released are small and remain almost invariable during Cu and Ni adsorption for the initial concentrations studied, indicating that they were not affected by the Cu and Ni adsorption. On the other hand, the amounts of the Ca^{2+} and Mg^{2+} ions released from the surfaces of both clays are greater, with the total released Ca^{2+} and Mg^{2+} contents from sample VRM being significantly greater than those from ATP. This is in accordance with the experimental results which showed higher adsorption capacity of the VRM for Cu^{2+} and Ni^{2+} ions than the ATP. The amounts of both Ca^{2+} and Mg^{2+} released from palygorskite increased with increasing initial metal concentration, while in vermiculite an increase in mainly Mg^{2+} ions was observed. The main reason for the increase in the release of Ca^{2+} and Mg^{2+} is the larger amounts of adsorbed Cu^{2+} and Ni^{2+} ions on the two clays by increasing their initial metal concentrations. Both clay adsorbents adsorbed successfully even higher Cu^{2+} and Ni^{2+} concentrations with simultaneous increase in Ca^{2+} and/or Mg^{2+} release.

In all studied cases, more cations were released than were metals adsorbed, indicating that ion-exchange reactions were more likely to predominate in Cu^{2+} and Ni^{2+} adsorption by both palygorskite and vermiculite (Fig. 9). Moreover, taking into account the CEC values of the natural clays (~0.58 meq/g for ATP and ~1.28 meq/g for VRM), it was clear that saturation was not reached. This observation indicated that Cu^{2+} and Ni^{2+} species occupy the exchange sites, forcing directly the release of counterbalanced ions through an ion exchange process and form outer-sphere complexes (Stumm, 1991):

$$(\equiv S-O^-)_2...C^{n+}_{3-n} + M^{2+} \rightleftharpoons (\equiv S-O^-)_2...M^{2+} + (3-n)C^{n+},$$

where S corresponds to framework Si or Al, C is the counterbalanced ion with charge n^+ ($n = 1$ or 2) and M is the studied metal Cu^{2+} or Ni^{2+}.

A more detailed analysis of the chemical compositions of the surfaces of the natural clays used and the presence of Cu and Ni were investigated by elemental mapping using energy dispersive X-ray (EDX) (Fig. 10). The Si, Al, Fe and Mg corresponding micrographs for the two natural clays indicated the distribution of the functional groups formed on the surface. The presence of copper and nickel adsorbed on attapulgite and vermiculite showed uniform distribution in all cases (Fig. 10).

CONCLUSIONS

The present work aimed to study the use of a set of natural, low-cost clays in their capacity to adsorb Cu^{2+} and Ni^{2+} ions for environmental applications. Parameters that affect the ability of vermiculite and palygorskite to remove Cu and Ni were evaluated and the mechanistic model that best describes the process was determined. The experimental results indicated that adsorption of Cu^{2+} and Ni^{2+} ions by the studied clays was heavily dependent on pH, while an increase in mineral amount increased in turn the removal percentage. The adsorption kinetics were rapid with equilibrium being established in ~60 min and followed the pseudo-second-order kinetic model. The adsorption isotherms were better simulated by the Langmuir model with the exception of Cu^{2+} adsorption to vermiculite which was better fitted by the Freundlich model. The maximum adsorption capacities for Cu^{2+} were 12.53 mg g^{-1} and 32.68 mg g^{-1} for palygorskite and vermiculite, respectively, while the corresponding values for Ni^{2+} ions were 11.57 mg g^{-1} and 37.85 mg g^{-1}, respectively. The proposed ion-exchange mechanism was verified indirectly by the fact that a gradual increase of exchangeable Ca^{2+} and Mg^{2+} ions was followed by an increase in the adsorption capacity with increasing initial concentration.

https://doi.org/10.1180/clm.2017.1 Published online by Cambridge University Press

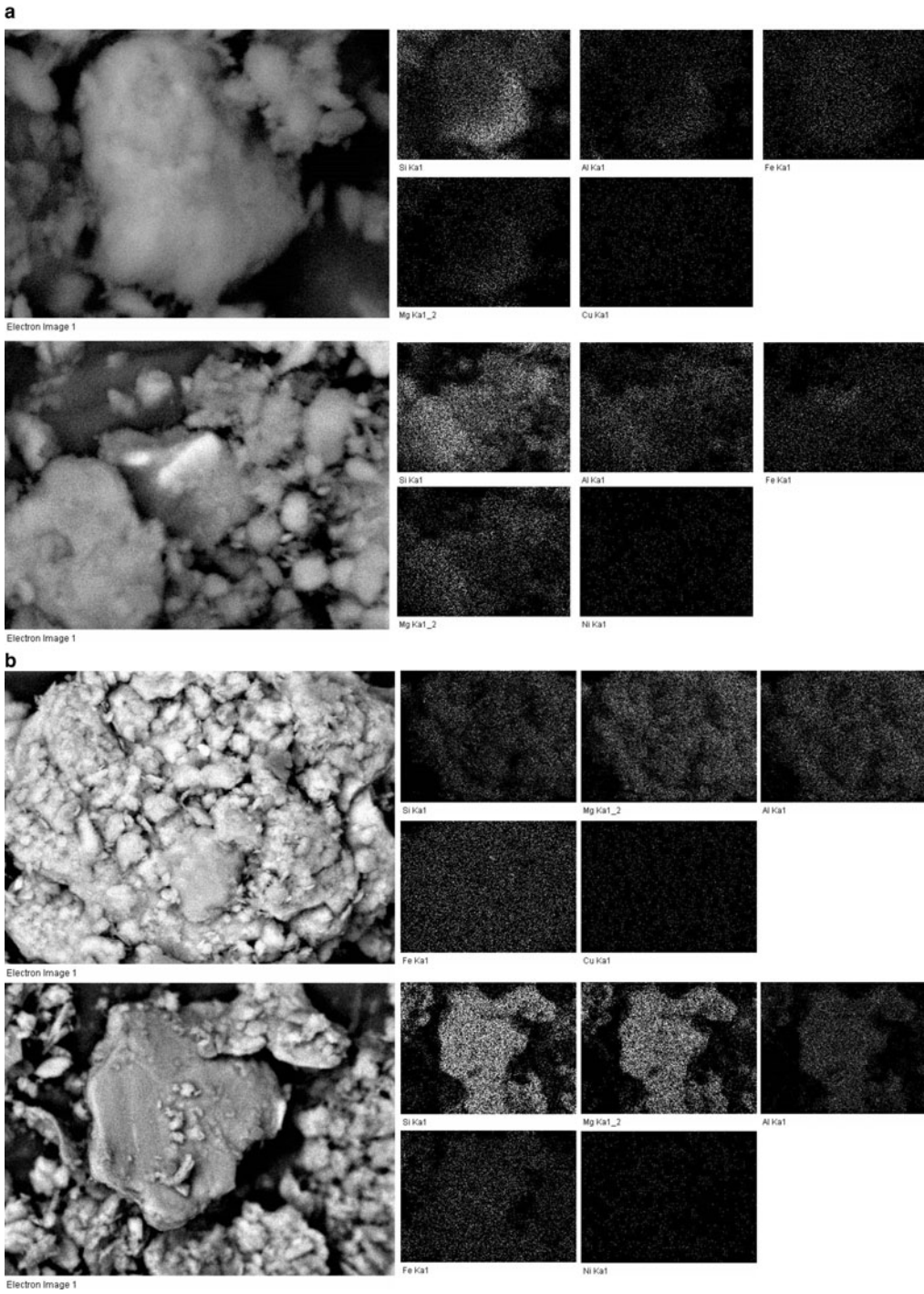

FIG. 10. SEM-EDX mapping images of the natural clays studied after (a) Cu^{2+} and (b) Ni^{2+} adsorption.

https://doi.org/10.1180/clm.2017.1 Published online by Cambridge University Press

ACKNOWLEDGMENTS

Part of this study was co-financed by the European Union (European Social Fund – ESF) and Greek national funds through the Operational Program "Education and Lifelong Learning" of the National Strategic Reference Framework (NSRF) – Research Funding Program: Heraclitus II: Investing in knowledge society through the European Social Fund. The authors extend their thanks to the Greek local authorities in the regions of western and central Macedonia, Greece, for procedural facilitation with raw material collection.

REFERENCES

Abollino O., Giacomino A., Malandrino M. & Mentasi E. (2008) Interaction of metal ions with montmorillonite and vermiculite. *Applied Clay Science*, **38**, 227–236.

Al-Makhadmeh L. & Batiha M.A. (2016) Removal of iron and copper from aqueous solutions using Jordanian kaolin and zeolitic tuff. *Desalination and Water Treatment*, **57**, 20930–20943.

Alexiades C.A. & Jackson M.L. (1966) Quantitative clay mineralogical analysis of soils and sediments. *Clays and Clay Minerals*, **14**, 35–52.

Alvarez-Ayuso E. & Garcia-Sanchez A. (2003) Removal of heavy metals from wastewaters by natural and Na-exchanged bentonites. *Clays and Clay Minerals*, **51**, 475.

Baker H. (2009) Characterization for the interaction of nickel(II) and copper(II) from aqueous solutions with natural silicate minerals. *Desalination*, **244**, 48–58.

Bayat B. (2002) Comparative study of adsorption properties of Turkish fly ashes I. The case of nickel (II), copper(II) and zinc(II). *Journal of Hazardous Materials*, **B10**, 285–300.

Bhattacharya A.K., Mandal S.N. & Das S.K. (2006) Adsorption of Zn (II) from aqueous solution by using different adsorbents. *Journal of Chemical Engineering*, **123**, 43–51.

Bourliva A., Michailidis K., Sikalidis C. & Filippidis A. (2013a) Spectroscopic and thermal study of bentonites from Milos Island, Greece. *Bulletin of the Geological Society of Greece*, **47**, 2020–2029.

Bourliva A., Michailidis K., Sikalidis C., Filippidis A. & Betsiou M. (2013b) Lead removal from aqueous solutions by natural Greek bentonites. *Clay Minerals*, **48**, 771–787.

Bourliva A, Michailidis K., Sikalidis C., Filippidis A. & Betsiou M. (2015) Adsorption of Cd(II), Cu(II), Ni(II) and Pb(II) onto natural bentonite: study in mono- and multi-metal systems. *Environmental Earth Science*, **73**, 5435–5444.

Brewer G.J. (2003) Copper in medicine. *Current Opinion in Chemical Biology*, **7**, 207–212.

Brewer G.J. (2014) The promise of copper lowering therapy with tetrathiomolybdate in the cure of cancer and in the treatment of inflammatory disease. *Journal of Trace Elements in Medicine and Biology*, **28**, 372–378.

Chahi A., Petit S. & Decarreau A. (2002) Infrared evidence of dioctahedral-trioctahedral site occupancy in palygorskite. *Clays and Clay Minerals*, **50**, 306–313.

Cheremisinoff P.N. (1995) *Handbook of Water and Wastewater Treatment Technology*. Marcel Dekker Inc., New York.

Christidis G.E., Katsiki P., Pratikakis A. & Kacandes G. (2010) Rheological properties of palygorskite-smectite suspensions from the Ventzia basin, W. Macedonia, Greece. *Bulletin of the Geological Society of Greece*, **43**, 2562–2569.

Covelo E.F., Vega F.A. & Andrade M.L. (2007) Competitive sorption and desorption of heavy metals by individual soil components. *Journal of Hazardous Materials*, **140**, 308–315.

De Pablo L., Chavez M.L. & Abatal M. (2011) Adsorption of heavy metals in acid to alkaline environments by montmorillonite and Ca-montmorillonite. *Journal of Chemical Engineering*, **171**, 1276–1286.

Ding S., Sun Y., Yang C. & Xu B. (2009) Removal of copper from aqueous solutions by bentonites and the factors affecting it. *International Journal of Mining Science and Technology*, **19**, 489–492.

El-Bayaa A., Badawy N. & Abd Alkhalik E. (2009) Effect of ionic strength on the adsorption of copper and chromium ions by vermiculite pure clay mineral. *Journal of Hazardous Materials*, **170**, 1204–1209.

Eren E. & Afsin B. (2008) An investigation of Cu(II) adsorption by raw and acid-activated bentonite: A combined potentiometric, thermodynamic, XRD, IR, DTA study. *Journal of Hazardous Materials*, **151**, 682–691.

Eren E. (2008) Removal of copper ions by modified Unye clay, Turkey. *Journal of Hazardous Materials*, **159**, 235–244.

Frost R.L., Locos O.B., Ruan J. & Kloprogge J.T. (2001) Near-infrared and mid-infrared spectroscopic study of sepiolites and palygorskites. *Vibrational Spectroscopy*, **27**, 1–13.

Fu F. & Wang Q. (2011) Removal of heavy metal ions from wastewaters: A review. *Journal of Environmental Management*, **92**, 407–418.

Giles C.H., Smith D. & Huitson A. (1974) A general treatment and classification of the solute adsorption isotherm: I. Theoretical. *Journal of Colloid and Interface Science*, **47**, 755–765.

Harris E.D. (2003) Basic and clinical aspects of copper. *Critical Reviews in Clinical Laboratory Sciences*, **40**, 547–586.

Ho Y.S. & McKay G. (1998) A comparison of chemisorption kinetic models applied to pollutant removal on various sorbents. *Process Safety and Environmental Protection*, **76**, 332–340.

https://doi.org/10.1180/clm.2017.1 Published online by Cambridge University Press

Hojati S. & Landi A. (2015) Kinetics and thermodynamics of zinc removal from a metalplating wastewater by adsorption onto an Iranian sepiolite. *International Journal of Environmental Science and Technology*, **12**, 203–210.

Hu H. (2002) Human health and heavy metals exposure. In: *Life Support: The Environment and Human Health* (M. McCally, editor). MIT Press, Cambridge, Massachusetts, USA.

Ijagbemi C.O., Baek M. & Kim D. (2009) Montmorillonite surface properties and sorption characteristics for heavy metal removal from aqueous solutions. *Journal of Hazardous Materials*, **166**, 538–546.

Ijagbemi C.O., Baek M. & Kim D. (2010) Adsorptive performance of un-calcined sodium exchanged and acid modified montmorillonite for Ni^{2+} removal: Equilibrium, kinetics, thermodynamics and regeneration studies. *Journal of Hazardous Materials*, **174**, 745–755.

Jiang M., Jin X., Lu X. & Chen Z. (2010) Adsorption of Pb(II), Cd(II), Ni(II) and Cu(II) onto natural kaolinite clay. *Desalination*, **252**, 33–39.

Kastritis I.D., Kacandes G.H. & Mposkos E. (2003) The palygorskite and Mg-Fe-smectite clay deposits of the Ventzia basin, western Macedonia, Greece. In: *Proceedings of the 7th SGA-Mineral Exploration and Sustainable Development Meeting* (D.G. Eliopoulos, editor), Millpress, Rotterdam.

Kurniawan T.A., Chan G.Y.S., Lo W.H. & Babel S. (2006) Comparisons of low-cost adsorbents for treating wastewaters laden with heavy metals. *Science of the Total Environment*, **366**, 409–426.

Liu Z. & Zhou S. (2010) Adsorption of copper and nickel on Na-bentonite. *Process Safety and Environmental Protection*, **88**, 62–66.

Madejová J. & Komadel P. (2001) Baseline studies of the Clay Minerals Society Source Clays: infrared spectroscopy. *Clays and Clay Minerals*, **49**, 410–432.

Madejová J., Balan E. & Petit S. (2011) Application of vibrational spectroscopy to the characterization of phyllosilicates and other industrial minerals. In: *Advances in the Characterization of Industrial Minerals* (G.E. Christidis, editor), EMU Notes in Mineralogy, **9**, European Mineralogical Union and the Mineralogical Society of Great Britain and Ireland, London.

Magave R., Zhao J., Bowman L. & Ding M. (2012) Genotoxicity and carcinogenicity of cobalt-, nickel- and copper-based nanoparticles. *Experimental and Therapeutic Medicine Journal*, **4**, 551–561.

Malamis S. & Katsou E. (2013) A review on zinc and nickel adsorption on natural and modified zeolite, bentonite and vermiculite: Examination of process parameters, kinetics and isotherms. *Journal of Hazardous Materials*, **252–253**, 428–461.

Mathialagan T. & Viraraghavan T. (2003) Adsorption of cadmium from aqueous solutions by vermiculite. *Separation Science and Technology*, **38**, 57–76.

Mendelovici E. (1973) Infrared study of attapulgite and HCl treated attapulgite. *Clays and Clay Minerals*, **21**, 115–119.

Muiambo H.F., Focke W.W., Atanasova M., Van Der Westhuizen I. & Tiedt L.R. (2010) Thermal properties of sodium-exchanged Palabora vermiculite. *Applied Clay Science*, **50**, 51–57.

Murray H.H. (1999) Applied clay mineralogy today and tomorrow. *Clay Minerals*, **34**, 39–49.

Ozdemir G. & Yapar S. (2009) Adsorption and desorption behavior of copper ions on Na-montmorillonite: effect of rhamnolipids and pH. *Journal of Hazardous Materials*, **166**, 1307–1313.

Potgieter J.H., Potgieter-Vermaak S.S. & Kalibantonga P.D. (2006) Heavy metals removal from solution by palygorskite clay. *Minerals Engineering*, **19**, 463–470.

Sdiri A.T., Higashi T. & Jamoussi F. (2014) Adsorption of copper and zinc onto natural clay in single and binary systems. *International Journal of Environmental Science and Technology*, **11**, 1081–1092.

Sen Gupta S. & Bhattacharyya K.G. (2008) Immobilization of Pb(II), Cd(II) and Ni(II) ions on kaolinite and montmorillonite surfaces from aqueous medium. *Journal of Environmental Management*, **87**, 46–58.

Sen T.K. & Gomez D. (2011) Adsorption of zinc (Zn^{2+}) from aqueous solution on natural bentonite. *Desalination*, **267**, 286–294.

Sharma A.D. (2006) Disulfiram and low nickel diet in the management of hand eczema: A clinical study. *Indian Journal of Dermatology, Venereology and Leprology*, **72**, 113–118.

Sharma A.D. (2013) Low nickel diet in dermatology. *Indian Journal of Dermatology*, **3**, 240.

Shukla A., Zhang Y.H., Dubey P., Margrave J.L. & Shukla S.S. (2002) The role of sawdust in the removal of unwanted materials from water. *Journal of Hazardous Materials*, **95**, 137–152.

Srinivasan R. (2011) Advances in application of natural clay and its composites in removal of biological, organic, and inorganic contaminants from drinking water. *Advances in Materials Science and Engineering*, **2011**, 1–17.

Srivastava V.C., Mall I.D. & Mishra I.M. (2008) Removal of cadmium(II) and zinc(II) metal ions from binary aqueous solution by rice husk ash. *Colloids and Surfaces A: Physicochemical and Engineering Aspects*, **312**, 172–184.

Stumm W. (1991) *Chemistry of the Solid–Water Interface*. J. Wiley & Sons Inc, New York.

Stylianou M.A., Inglezakis V.J., Moustakas K.G., Malamis S.P. & Loizidou M.D. (2007) Removal of Cu(II) in fixed bed and batch reactors using natural zeolite and exfoliated vermiculite as adsorbents. *Desalination*, **215**, 133–142.

Suárez M. & García-Romero E. (2006) FTIR spectroscopic study of palygorskite: Influence of the

https://doi.org/10.1180/clm.2017.1 Published online by Cambridge University Press

composition of the octahedral sheet. *Applied Clay Science*, **31**, 154–163.

Tahir S. & Rauf N. (2003) Thermodynamic studies of Ni(II) adsorption onto bentonite from aqueous solution. *The Journal of Chemical Thermodynamics*, **35**, 2003–2009.

Tang P., Chew N.Y., Chan H.K. & Raper J.A. (2003) Limitation of determination of surface fractional dimension using N_2 adsorption isotherms and modified Frenkel-Halsey-Hill theory. *Langmuir*, **19**, 2632–2638.

Tsirambides A. & Michailidis K. (1999) An X-ray, EPMA, and oxygen isotope study of vermiculitized micas in the ultramafic rocks at Askos, Macedonia, Greece. *Applied Clay Science*, **4**, 121–140.

Uddin M.K. (2017) A review on the adsorption of heavy metals by clay minerals, with special focus on the past decade. *Chemical Engineering Journal*, **308**, 438–462.

Veli S. & Alyüz B. (2007) Adsorption of copper and zinc from aqueous solutions by using natural clay. *Journal of Hazardous Materials*, **149**, 226–233.

Xueyi G. & Inoue K. (2003) Elution of copper from vermiculite with environmentally benign reagents. *Hydrometallurgy*, **70**, 9–21.

Yavuz O., Altunkaynak Y. & Güzel F. (2003) Removal of copper, nickel, cobalt and manganese from aqueous solution by kaolinite. *Water Research*, **37**, 948–952.

https://doi.org/10.1180/clm.2017.1 Published online by Cambridge University Press